Intergranular Corrosion in Stabilized 310 Stainless Steel

AUTHOR(S):

VISITSERNGTRAKUL, Supapan; HASHIMOTO, Satoshi; MIURA, Sei; OKUBO, Masao

CITATION:

VISITSERNGTRAKUL, Supapan ...[et al]. Intergranular Corrosion in Stabilized 310 Stainless Steel. Memoirs of the Faculty of Engineering, Kyoto University 1990, 52(2): 68-80

ISSUE DATE:

1990-04-30

URL:

http://hdl.handle.net/2433/281414

Intergranular Corrosion in Stabilized 310 Stainless Steel

by

Supapan VISITSERNGTRAKUL[$], Satoshi HASHIMOTO[*],
Sei MIURA[*] and Masao OKUBO[**]

(Received December 20, 1989)

Abstract

The intergranular corrosion in stabilized 310 stainless steel polycrystals has been investigated from a view point of crystallographic structure of the grain boundary. The relative orientation of each grain was characterized by the Coincidence Site Lattice (CLS) model, and the Plane Matching model. For the quantitative characterization of corrosion, a scanning electron microscope with two secondary electron detectors was used to provide the profile of the corrosion groove. It was found that $\Sigma = 3$ boundaries and some certain CSL boundaries have a high resistance against the intergranular corrosion. The "random" boundaries were corroded in a different extent, particularly high corrosivity. It is concluded that the grain boundaries having low Σ-values do not necessarily provide low corrosivity. It is shown that the dissolution rate depending on the surface orientation of grains also plays an important role in the morphology of intergranular corrosion, and was found to be lowest at (100) and increases as the surface normal changes towards (110), and more so towards (111).

1. Introduction

In certain environments, corrosion of stainless teel occurs predominantly at the grain boundaries (intergranular corrosion) which results in a loss of strength and ductility. The relative crystallographic orientation of both sides of a grain boundary is known to influence the rate of the intergranular corrosion.

---

* Department of Engineering Science, Feculty of Engineering, Kyoto University, Kyoto-606, Japan.

** Materials Research Group, Ehime Works, Sumitomo Chemical Co. Ltd., Niihama-792, Japan.

$ On leave from the School of Energy and Materials, King Mongkut's Institute of Technology Thonburi, Bangkok, Thailand. Research fellow supported by the Scholarship from The Ministry of Education, Science and Culture, Japan.

Several aspects of this phenomenon on various types of stainless steel have been investigated. Streicher [1] demonstrated the effect of cations in the corroding acids and the influence of heat treatment and grain size of the steel on the intergranular corrosion. Aust and his colleagues [2, 3, 4, 5, 6] have extensively studied the effect of heat treatment and of solute segregation with emphasis on the electrochemical mechanisms and segregation theory. Joshi and Stein [7] examined austenitic stainless steel with Auger electron spectroscopy, and found that in highly oxidizing solutions the impurity segregation and not the chromium depletion best explains the deterioration of the material properties. In all of these studies the degree of corrosion was measured in terms of the average weight loss of an entire specimen with little concern for crystallographic aspects.

Studies by Beaunier, Froment and Vignaud [8, 9], however, have used the orientation controlled bicrystals of stainless steel in order to find out the influence of the electrochemical condition and the impurity segregation. Sato et al. [10] reported that some coincidence boundaries and low angle boundaries showed low corrosivity in 304 stainless steel having 〈100〉-oriented coarse columnar grains. Bennett [11] recently showed some relationships between the disorientation angle and the average width of grain boundary groove in ferritic and austenitic stainless steel polycrystals. However, the disorientation angle (defined as the smallest rotation angle calculated from the rotational matrices which give an identical orientation relationship [12]) is not an appropriate parameter to describe the grain boundary structure. More precise and quantitative studies in polycrystals which contain various structures of grain boundaries are required.

The purpose of the present investigation is to clarify the influence of the grain boundary structure described in terms of Σ-values, using the Coincidence Site Lattice (CSL)# concept on the corrosivity from the characterized individual profile of the corroded groove. The effect of the surface normal orientation of each grain on the dissolution rate is also taken into account.

The relative orientation of the lattice on both sides of a grain boundary is described by a rotational pattern in three dimensions that makes a certain fraction of lattice points in this Coincidence Site Lattice (CSL) coincide. The Σ-value is the reciprocal of this fraction.

2. Experimental Method

2.1 Specimen Preparation

Specimens of type 310 stainless steel containing Nb of dimension 20 × 25 × 5 mm^3 were prepared by the strain-annealing method at 2% elongation, 1350℃ for 30 minutes to obtain large grain sizes for the convenience of the crystallographic analysis. It was confirmed that these specimens are nonsensitized because there is no chromium cabide precipitation at the grain boundary. The average grain size is about 600 μm. The chemical composition of the material is given in Table 1. The grain boundary features were revealed by mechanical polishing with emery papers #600, #800, #1000 and diamond paste 2.5 μm diameter, subsequent electro-polishing with 10% oxalic acid at room temperature at 18 V for 90 sec, followed by light electroetching at 4 V for 20 sec.

Table 1 Composition of Stabilized 310 Stainless Steel Used (wt. %).

Cr	Ni	C	O	N	P	S	Si	B	Sn
24.85	20.27	0.011	0.0077	0.0232	0.019	0.0004	0.26	0.0001	0.002

Al	Cu	Co	Nb	Mo	Mn	V	rem	Fe
0.010	0.03	0.36	0.24	0.03	0.67	0.068	0.014	balance

rem=rare earth metals

2.2 Analysis of the Crystallographic Structure of the Grain Boundary.

The crystallographic orientation of each grain was obtained by analyzing the Back-Reflection X-ray Laue pattern using a system automated by a microcomputer [13]. The deviation angle from the nearest CSL-orientation was calculated by comparing the actual orientation relation with the ideal CSL-orientation.

The orientation relations from $\Sigma = 1$ to $\Sigma = 101e$ in the CSL system were considered. The allowable deviation ($\Delta\theta_c$) from the nearest CSL-orientation that can be accommodated by grain boundary dislocations was taken to be $\Delta\theta_c = 15(\Sigma)^{-1/2}$ degrees as proposed by Brandon [14]. The grain boundary which can be defined by the Plane Matching* model [15] is called "PM". The boundary that does not meet the above criteria is called "random" boundary, R.

---

* Plane matching model is defined for the grain boundary across which at least a single set of crystallographic low-index planes is continuous. The grain boundaries having deviation angles less than 5 degrees from the ideal PM relation are considered in this study.

2.3 Corrosion Test and Measurement

The specimen was subsequently corroded in 200 ml of boiling 5 N nitric acid containing 3 g/ l of potassium dichromate to accelerate the corrosion rate. The concentration of the solution was maintained by a reflux condenser. The quantitative measurement was mainly conducted by a scanning electron microscope with two secondary electron detectors (Elionix, EMM 3000, Electron beam diameter 10 nm, resolution: lnm and 10 nm in the directions parallel and perpendicular to the surface, respectively.) [16], so that the profile of the corroded groove can be obtained. In some cases the measurement was carried out by light-focusing, and by an interference method. The corrosion test should not proceed too long because the surface becomes rough and the groove too deep. It was found by preliminary tests that 20 minutes corrosion was suitable for the investigation.

3. Experimental Results

3.1 The Distribution of Σ-values

The relative orientation of the adjacent grains in terms of the disorientation angle and axis is given in Table 2. There are three possible Σ-values for the orientation relation between grains #33 and #36, i. e. Σ= 13 b, 21 a and 67 a. The deviation angles of all three Σ-values are smaller than the allowable deviation angles. It is noted that the proper Σ-value can not be determined without observation of, at least, the configuration of the grain boundary dislocation [17].

The distribution of Σ-values of the analyzed grain boundaries (including annealing twin bands) is shown as histogram in Fig. 1. It was found that a half of the boundaries were of $\Sigma \leqslant 101$. The most frequently observed value (30%) is Σ= 3 of which approximately half were associated with twin boundaries (shaded area in histogram). The PM boundaries were observed with the frequency of 11%. Most of them have the deviation anle within 1.5 degrees. All of the matching planes are not parallel to the grain boundary except one case. Four out of eight have a matching plane of (111)//(100), three of the (111)//(110) and one of the (111)//(111). In every case, one of the low index planes is the (111) plane.

The ratio of length of each coincidence boundary to the total length of the grain boundaries examined is also shown at the right hand column of each Σ-value in Fig. 1. It is obvious that even though the number of Σ= 3 boundaries is less than that of the random boundaries, the length of Σ= 3 is larger. Every Σ= 3 grain boundary was found to possess the common plane (111).

Table 2.1 Grain Boundary Character of the CSL-Related Grain Boundary and Corroded Groove Depth.

Grain No.	Adjacent Grain No.	Σ-value	Grain Boundary Character			Corroded Goove Depth
			Deviation	Disorientation		
			angle, $\Delta\theta°$	Angle, $\theta°$	Axis	μm
1	2	3	1.22	58.91	.584, .578, .570	*
5	6	3	0.71	60.48	.585, .574, .573	*
8	39	3	0.59	59.60	.583, .577, .572	*
9	10	3	5.85	57.64	.623, .603, .498	*
11	12	3	1.33	59.82	.596, .572, .564	*
12	13	3	1.68	59.03	.596, .572, .563	*
26	27	3	0.67	59.74	.586, .573, .572	*
29	32	3	1.18	59.04	.587, .574, .571	*
34	35	3	0.54	59.46	.578, .578, .576	*
40	41	3	1.49	60.13	.598, .569, .564	7.3
40	42	3	1.51	59.15	.591, .580, .560	*
17	18	3t	0.72	59.32	.580, .578, .574	*
18	19	3t	0.31	59.73	.579, .578, .575	*
21	22	3t	0.67	60.64	.579, .578, .575	*
21	23	3t	0.67	60.64	.579, .578, .575	*
23	24	3t	0.67	60.64	.579, .578, .575	*
24	25	3t	0.67	60.64	.579, .578, .575	*
25	28	3t	0.67	60.64	.579, .578, .575	*
30	31	3t	0.34	59.76	.581, .576, .575	*
46	47	3t	0.55	59.87	.585, .574, .573	*
47	48	3t	0.28	59.89	.580, .579, .574	*
51	52	3t	0.58	59.93	.582, .580, .569	*
52	53	3t	0.98	60.30	.585, .583, .564	*
36	37	7	5.58	35.99	.630, .628, .457	7.5
11	13	9	0.48	39.37	.710, .704, .003	6.6
28	29	9	5.41	42.39	.762, ,644, .063	7.3
39	45	9	4.88	39.04	.766, .636, .088	7.6
22	57	11	3.87	47.69	.746, .666, .002	7.5
5	7	11	3.82	53.56	.723, .690, .039	*
33	36	13b	3.14	24.89	.605, .582, .543	*
		(21a	3.27			
		67a)	1.19			
53	54	15	1.98	47.92	.897, .441, .042	8.3
28	32	19a	3.81	28.77	.782, .623, .003	7.9
26	57	23	2.98	43.10	.901, .329, .282	7.8
27	28	25b	0.96	52.40	.690, .682, .240	7.8
27	57	25b	2.13	49.94	.695, .689, .205	7.8
1	53	27a	2.89	33.52	.735, .676, .053	8.6
29	30	57b	2.02	40.70	.771, .566, .290	7.2
26	28	75a	0.76	22.04	.906, .322, .274	7.7
52	56	87a	1.25	18.65	.876, .482, .028	7.2
1	54	101e	1.47	48.46	.715, .677, .172	7.3

* : no corroded groove at the grain boundary
3t : $\Sigma = 3$ annealing twin band

Table 2.2 Grain Boundary Character of the Plane Matching, PM and Random, R Boundary and Corroded Groove Depth.

Grain No.	Adjacent Grain No.	Σ=value	Grain Boundary Character			Corroded Groove Depth
			Parallelism	Disorientation		
				Angle, $\theta°$	Axis	
						μm
1	52	PM	(111)/(110)	36.46	.831, .544, .114	7.7
8	38	PM	(111)/(110)	37.45	.843, .527, .108	6.6
16	17	PM	(100)/(111)	56.55	.734, .526, .429	7.7
20	21	PM	‡(111)/(100)	57.53	.782, .584, .216	7.4
29	33	PM	(111)/(100)	52.83	.753, .654, .065	7.8
42	44	PM	(111)/(110)	40.54	.808, .578 .114	7.8
49	50	PM	(111)/(100)	55.83	.744, .663, .086	7.8
51	55	PM	(111)/(111)	51.03	.621, .561, .547	8.5
6	7	R	—	17.50	.733, .665, .143	*
8	40	R	—	46.54	.928, .373, .016	7.3
15	16	R	—	20.19	.891 .434, .135	7.9
15	17	R	—	58.71	.758, .630, .169	7.7
15	18	R	—	25.56	.903, .429, .004	7.7
15	22	R	—	43.08	.714, .683, .153	8.1
19	20	R	—	53.32	.764, .623, .167	7.6
20	22	R	—	48.00	.831, .409, .378	7.4
20	23	R	—	48.00	.831, .409, .378	7.4
26	30	R	—	47.74	.832, .438, .342	7.4
28	57	R	—	33.40	.941, .267, .209	7.7
29	31	R	—	54.78	.719, .562, .409	8.8
29	34	R	—	32.09	.742, .611, .276	7.8
29	35	R	—	47.11	.839, .539, .079	7.8
30	32	R	—	46.20	.843, .520, .138	7.8
38	39	R	—	33.19	.942, .274, .193	7.8
39	40	R	—	39.21	.731, .624, .274	7.8
39	42	R	—	49.25	.642, .573, .509	7.9
39	44	R	—	36.61	.836, .398, .377	7.7
42	43	R	—	37.45	.974, .223, .042	8.1
43	44	R	—	34.42	.731, .626, .271	7.8
45	46	R	—	58.63	.767, .625, .144	7.4
47	50	R	—	44.39	.811, .583, .051	7.7
48	49	R	—	52.78	.788, .478, .388	7.6
48	50	R	—	27.96	.861, .501, .084	7.8
50	55	R	—	52.77	.654, .564, .504	8.0
51	56	R	—	58.77	.722, .634, .278	8.6

* : no corroded groove at the grain boundary.
‡ : the matching planes are parallel to the grain boundary.

3.2 Corrosion Features

A typical example of intergranular corrosion of stabilized 310 stainless steel sample after immersion for three hours in the nitric-dichromate solution is shown in Fig. 2, demonstrating that the corrosion resistance differs among the grain boundaries.

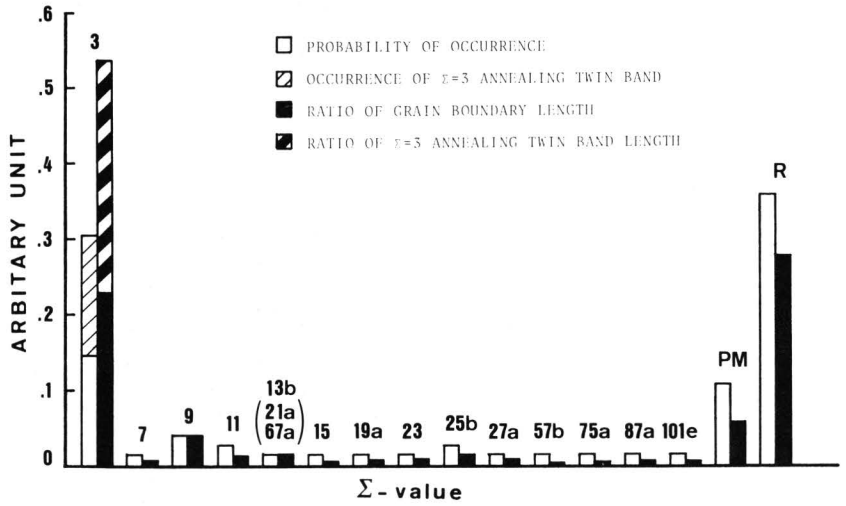

Fig. 1 Probability of occurrence of CSLs and the ratio of length of each coincidence boundary to the total length of grain boundaries examined in stabilized 310 stainless steel polycrystal.

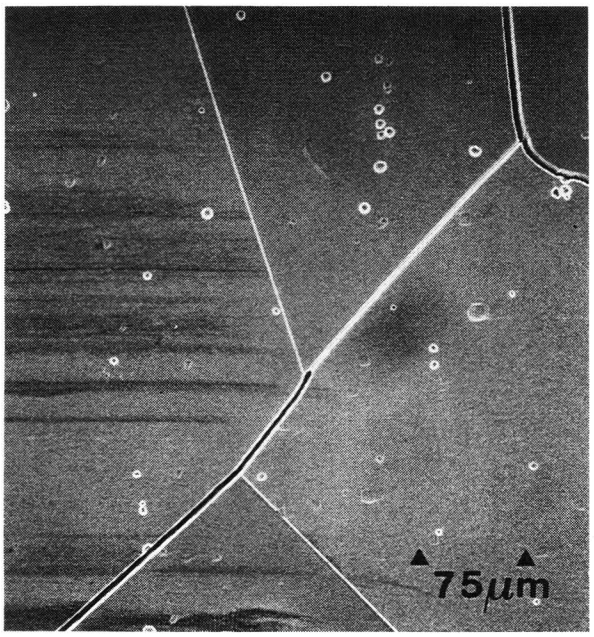

Fig. 2 A typical example of intergranular corrosion of stabilized 310 stainless steel showing the differences in corrosion of different grain boundries after immersion for three hours in nitric-dicromate solution.

Profiles of the corroded grooves of grain boundaries having different Σ-values are shown in Fig. 3. It is apparent that the $\Sigma=3$ houndary has no groove, while the $\Sigma=25$ b and the random boundaries have grooves of a different extent. The significant difference of the surface levels between the adjacent grains can also be clearly observed.

The difference of the surface levels of the adjacent grains after corrosion was measured then converted to the dissolution rate and presented as an anisotropic line in the standard triangle as shown in Fig. 4. The points inside the triangle correspond to the projection of the surface normal orientations of the grains measured. The number outside the triangle is the dissolution rate in μm/min.

The corroded groove depth which is measured from the original level, d, not $h_A$or h_B (see Fig. 5) is defined as a parameter to describe the corrosivity because the dissolution rate of the grain surface depends strongly on the crystallographic orientation. The value *"d"* of eack corroded groove was determined by the following equation:

$$d=h_A+d_C+d_{100}$$

h_A : the distance from the bottom of the groove to the lower surface level.

d_c : the distance from the lower surface level to the surface level of grain orienting (100). This value was taken from the standard triangle when the surface normal of each grain was known.

d_{100} : the distance from the surface level of grain orienting (100) to the original level. The calculation process is as follow:
The difference of the surface level between (100) and (111) was measured to be 4μm.

$$d_{100}-d_{111}=-4\mu m$$

The mean corrosion distance, d_m which was calculated from the weight loss and the surface area change during the corrosion process was 7.5μm.

$$(d_{100}+d_{111})/2=7.5\mu m$$

Finally, d_{100} was calculated to be 5.5μm.

The result of the corrosion attack at each grain boundary is presented in the last column of Table 2 and categorized in Table 3. The effect of the deviation from CSL-related orientation on the corrosivity can not be deduced from the present results. It was found that the $\Sigma=3$ grain boundary, including $\Sigma=3$

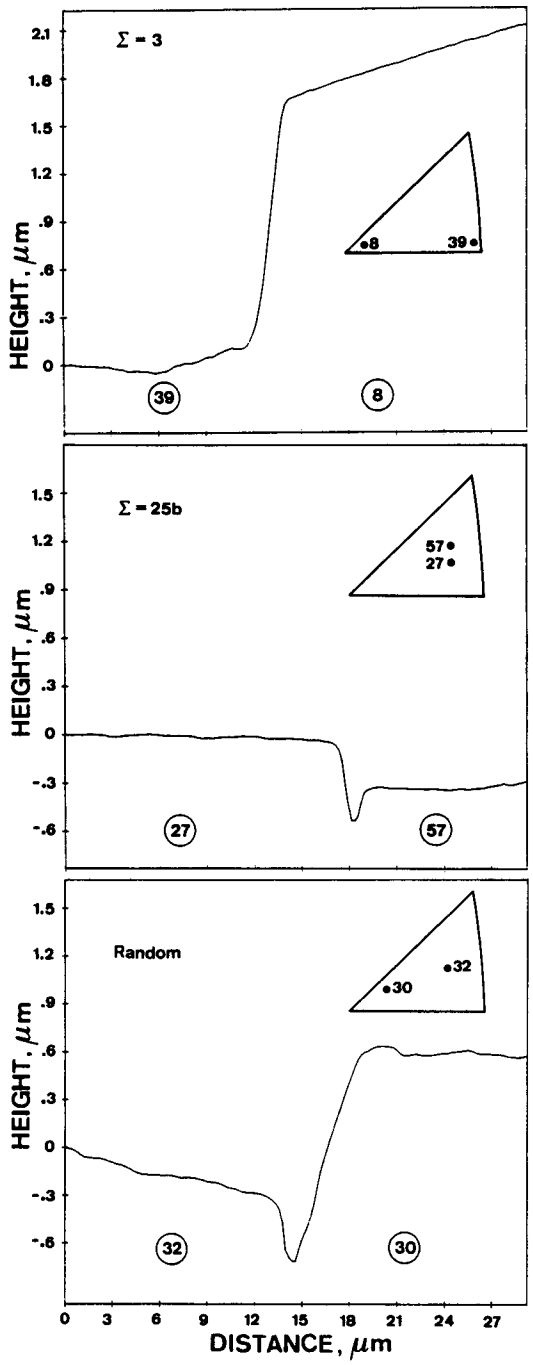

Fig. 3 Profiles of corrosion grooves for the $\Sigma=3$, $\Sigma=25b$ and a "random" boundary, respectively. The surface orientations of adjacent grains are also shown.

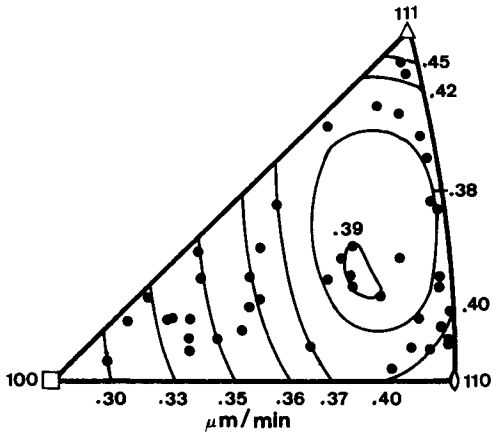

Fig. 4 A standard triangle showing the distribution of the surface normal of the examined specimen. Contour shows the surface dissolution rate (μm/min).

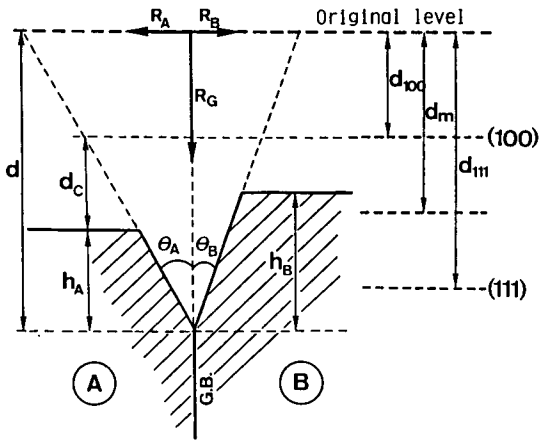

Fig. 5 Schematic feature of corroded groove showing the definition of corrosion depth (d), angles of groove wall from either side (θ_A, θ_B).

(111) coherent boundaries in annealing twin bands, resists most strongly to the intergranular corrosion, and no groove is formed. The $\Sigma s = 7$ and 9 boundaries are slightly corroded. Other coincidence boundaries are apparently more corroded, except for $\Sigma s = 11$ and 13 b (21 a, 67 a). The PM boundaries show almost the same tendency of the corrosivity as the random ones.

Table 3 Summary of the Grain Boundary Corrosivity

Σ-value	n	Corrosivity					Total number
		a	b	c	d	e	
3	10		1				11
3t	12						12
7			1				1
9		1	1	1			3
11	1		1				2
13b (21a, 67a)	1						1
15					1		1
19a				1			1
23				1			1
25b				2			2
27a						1	1
57b			1				1
75a				1			1
87a			1				1
101e			1				1
PM		1	1	5	1		8
R	1		5	17	2	2	27
Total	25	2	13	28	4	3	75

n: no groove b: $7.0<d\leqq7.5\,\mu m$ d: $8.0<d\leqq8.5\,\mu m$
a: $6.5<d\leqq7.0\,\mu m$ c: $7.5<d\leqq8.0\,\mu m$ e: $8.5<d\leqq9.0\,\mu m$
3 t: $\Sigma=3$ annealing twin band
PM: plane matching boundary
R: random boundary

4. Discussion

The most frequently observed grain boundary in the present investigation is $\Sigma=3$ (111) due to its low-energy structure as was found in Copper, Aluminium and Nickel [9, 18, 19, 20]. This is also supported by the fact that the total length of $\Sigma=3$ is much larger than the total length of the random boundaries in spite of the smaller number of the $\Sigma=3$ boundary. The common planes of all $\Sigma=3$ boundaries are of type (111), the most stable of the interfacial planes with a free energy of 19 erg/cm^2, as compared to 209 erg/cm^2 for an incoherent twin boundary, and to 835 erg/cm^2 for a random boundary [21].

Twin boundaries were observed in this study exclusively for $\Sigma=3$. This is in contrast with the work of Kopezky et al. [22] who obsersed annealing twin-shaped boundaries for $\Sigma s=5, 9, 11, 13, 17$ as well. No low-angle boundaries with $\Sigma=1$ were observed.

The results indicate that there exists a correlation between the degree of

intergranular corrosion and the crystallographic structure of the grain boundary. It is generally accepted that the low energy boundary will have a high resistance against corrosion [10, 18, 19]. However, the low Σ-value boundary does not always correlate with the low energy boundary as clearly shown by Herrmann et al. [18] and Goodhew [23]. The present investigation is in good agreement with the above studies. Some other coincidence boundaries having Σ-values such as $\Sigma s = 57$ b, 87 a, and 101 e were corroded less than the lower Σ-value boundaries: $\Sigma s = 15$, 19 a, 23, 25 b and 27 a. This is in contrast with the suggestion of Watanabe [24] that the boundary whose $\Sigma > 30$ will be classified as a "random" boundary and can be the preferential sites for corrosion and fracture.

The wall inclination of the corroded groove described by the angles θ_A, θ_B as shown in Fig. 5 can be estimated, based on the hypothesis that the dissolution rate along the grain boundary plane, R_G, and the dissolution rates of the grain boundary plane normals in grains A and B as R_A and R_B respectively, determine these inclination angles. However, the experimental results show that the dissolution rate of the grain boundary plane normals R_A and R_B is 2-4 times higher than the calculation. It is, therefore, supposed that there are some accelerated effects, e. g. the grain boundary structure itself and the segregation of impurity at the grain boundary that expedite the dissolution rate normal to the grain boundary plane. Consequently, it is apparent that the experimental results do not support this hypothesis.

The corrosion rate tended to be lowest for (100) and to increase for the surface normals near (110) and near (111) in sequence. The present result is simular to those in copper by Leidheiser and Gwathmey [25] and in aluminium by Arora and Metzger [26]. This tendency can not be explained in terms of the surface free energy, F_s, because $F_s(100)$ is larger than $F_s(111)$ in FCC metals [27]. It was supposed that the corrosion is viewed as the competitive process of the formation and breakdown of the passive film which is most stable on (100) [25, 28].

5. Conclusions

1. In stabilized 310 stainless steel polycrystals recrystallized by the strain annealing method, an abundance (30%) of $\Sigma = 3$ related coincidence boundaries including the coherent twin band was observed, followed by the other coincidence boundaries, $\Sigma \leqslant 101$ (23%) and the PM boundaries (11%).
2. The $\Sigma = 3$ boundaries and some CSL-related boundaries such as $\Sigma s = 11$, 13 b have the highest resistance against intergranular corrosion. It is emphasized

that only the Σ-value is not sufficient to describe the corrosivity.

3. The grains with a surface normal at (100) were found to have the lowest corrosion rate, which increases as the suface normal changes towards (110), and more so towards (111).

Achnowledgements–The authors wish to thank the Mechanical Engineering Research Laboratory, Kobe Steel, Ltd. for the facilities of plotting the corrosion-groove profile. Thanks are also due to Mr. R. Shimizu and Mr. T. Miyasaka for their valuable assistance.

References

1) M. A. Streicher; J. Electrochem. Soc; **106**, 161 (1959)
2) K. T. Aust, J. S. Armijo and J. H. Westbrook; Trans. ASM; **59**, 544 (1966)
3) K. T. Aust, J. S. Armijo, E. F. Koch and J. H. Westbrook; Trans. ASM; **60**, 360 (1967)
4) K. T. Aust, J. S. Armijo, E. F. Koch and J. H. Westbrook; Trans. ASM; **61**, 270 (1968)
5) K. T. Aust; Trans. AIME; **245**, 2117 (1969)
6) F. M. J. Morin and K. T. Aust; Can. Met. Quart.; **12**, 131 (1973)
7) A. Joshi and D. F. Stein; Corrosion; **28**, 321 (1972)
8) L. Beaunier, M. Froment and C. Vignaud; Phys. Chem. Solid State; Appl. to Metal and their Compounds, P. Lacombe ed., Elesevier, Amsterdam, p. 355 (1984)
9) M. Froment; J. Phys.; **36**, C 4-371 (1975)
10) A. Sato, K. Kon, S. Tsujikawa and Y. Hisamatsu; Tetsu to Hagane; **68**, 843 (1982)
11) B. W. Bennett; Pensylvania State University, Diss., 1984.
12) H. Grimmer; Acta Cryst.; **A 30**, 685 (1974)
13) O. Itoh, S. Hashimoto, S. Miura; J. Soc. Mat. Sci. Japan; **34**, 1105 (1985)
14) D. G. Brandon; Acta Metall.; **14**, 1479 (1966)
15) P. H. Pumphrey; Scripta Metall.; **6**, 107 (1972)
16) T. Suganuma; J. Electron Microsc.; **34**, 328 (1985)
17) C. Solenthaler and W. Bollmann; Mat. Sci. Eng.; **81**, 35 (1986)
18) G. Herrmann, H. Gleiter and G. Bäro; Acta Metall.; **24**, 353 (1976)
19) U. Erb, H. Gleiter and G. Schwitzgebel; Acta Metall.; **30**, 1377 (1982)
20) L. C. Lim and R. Raj; Acta Metall.; **32**, 1177 (1984)
21) L. E. Murr; Interfcial Phenomena in Metals and Alloys, Addison-wesley, 1975, p. 131
22) CH. V. Kopezky, V. Yu. Novikov, L. K. Fionova and N. A. Bolshakova; Acta Metall.; **33**, 873 (1985)
23) P. J. Goodhew; "Grain Boundary Structure and Kinetics", Amer. Soc. Metals, p. 155 (1980)
24) T. Watanabe; J. Phys.; **46**, C 4-555 (1985)
25) H. Leidheiser and A. T. Gwathmey; Trans. Electrochem. Soc.; **91**, 95 (1947)
26) O. P. Arora and M. Metzger; Trans. Metall. Soc. AIME; **236**, 1205 (1966)
27) L. E. Murr; in ref. 21, p. 53.
28) J. Ouder; Inter. Metals Rev.; **23**, 57 (1978)